

# A Posteriori Estimates for a Natural Neumann–Neumann Domain Decomposition Algorithm on a Unilateral Contact Problem

D. Choi, L. Gallimard, T. Sassi

► **To cite this version:**

D. Choi, L. Gallimard, T. Sassi. A Posteriori Estimates for a Natural Neumann–Neumann Domain Decomposition Algorithm on a Unilateral Contact Problem. *Journal of Scientific Computing*, Springer Verlag, 2015, 64 (3), pp.818 - 836. 10.1007/s10915-014-9944-8 . hal-01690027

**HAL Id: hal-01690027**

**<https://hal-univ-paris10.archives-ouvertes.fr/hal-01690027>**

Submitted on 22 Jan 2018

**HAL** is a multi-disciplinary open access archive for the deposit and dissemination of scientific research documents, whether they are published or not. The documents may come from teaching and research institutions in France or abroad, or from public or private research centers.

L'archive ouverte pluridisciplinaire **HAL**, est destinée au dépôt et à la diffusion de documents scientifiques de niveau recherche, publiés ou non, émanant des établissements d'enseignement et de recherche français ou étrangers, des laboratoires publics ou privés.

# A Posteriori Estimates for a Natural Neumann–Neumann Domain Decomposition Algorithm on a Unilateral Contact Problem

D. Choi · L. Gallimard · T. Sassi

Received: 11 December 2013 / Revised: 3 October 2014 / Accepted: 1 November 2014 /

Published online: 12 November 2014

© Springer Science+Business Media New York 2014

**Abstract** In this paper we present an error estimator for unilateral contact problems solved by a Neumann–Neumann Domain Decomposition algorithm. This error estimator takes into account both the spatial error due to the finite element discretization and the algebraic error due to the domain decomposition algorithm. To differentiate specifically the contribution of these two error sources to the global error, two quantities are introduced: a discretization error indicator and an algebraic error indicator. The effectivity indices and the convergence of both the global error estimator and the error indicators are shown on several examples.

**Keywords** Error estimation · Domain decomposition algorithm · Contact problem · Discretization error · Algebraic error

## 1 Introduction

In mechanical engineering, especially in structural analysis, multi-body contact problems are frequent. Contact is characterized by unilateral inequalities, describing the impossibility of tensile contact tractions, of material interpenetration and by an a priori unknown contact area. Combined with a finite element method (FEM), several approaches exist for solving the nonlinear equations issued from the discretization of frictionless contact problems [1–3]. An important point is to evaluate the approximation errors introduced by the numerical algorithm. For contact problems two distinct sources of errors are introduced: the first one due to the spatial discretization (the finite element mesh), the second one due to the algorithm used to solve the nonlinear equations. Several methods have been developed over many years to evaluate the global quality of FE analysis. For linear problems the earlier works have lead to estimators based on the residual of the equilibrium equation [4], estimators based

---

D. Choi (✉) · T. Sassi

LMNO – Université de Caen Basse-Normandie, Bld Maréchal Juin, 14032 Caen Cedex, France  
e-mail: daniel.choi@unicaen.fr

L. Gallimard

LEME, Université Paris Ouest Nanterre-La Défense, 50 rue de Sèvres, 92410 Ville d’Avray, France

on the concept of constitutive relation [5], and estimators using the smoothing of the finite element stresses [6]. For multi-body contact problems there is much less work [7–14]. A global error estimator in constitutive relation, which is an upper bound of the exact error, has been developed in [8] for unilateral contact problems without friction. This error estimate has been extended to friction problems in [10], to dynamic problems in [11] and to a natural Dirichlet–Neumann domain decomposition algorithm in [14]. An error estimate for linear elastic problems solved by FETI method [15] or BDD method [16] was proposed in [17].

In this paper, we consider a natural Neumann–Neumann Domain Decomposition (NNDD) algorithm, for two elastic bodies in contact, in which each iterative step consists of a Dirichlet problem for one body, a contact problem for the other one and two Neumann problems to coordinate contact stresses [19]. For the sake of simplicity, we shall here only consider two bodies contact problems where some Dirichlet conditions are imposed on each body.

The main objective of this paper is to present an a posteriori global error estimator for a frictionless contact problem, solved by a NNDD algorithm and two error indicators which allow to estimate the part of the error due to the spatial discretization and the part of the error due to the domain decomposition algorithm.

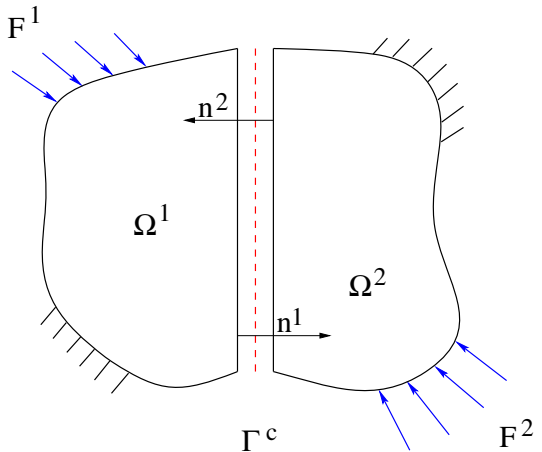
The paper is organized as follows: In Sect. 2, we introduce the frictionless contact problem to be solved. The domain decomposition algorithm is described in Sect. 3. In Sect. 4, the finite element variational formulations are introduced. Section 5 is devoted to the formulation of the global error estimator, the discretization error indicator and the algorithm error indicator. Finally, in Sect. 6, the different errors are analyzed through numerical examples.

## 2 Contact Problem

Let two elastic bodies, represented by  $\Omega^1$  and  $\Omega^2$ , be in unilateral contact along an interface  $\Gamma^c$ . Some displacements  $\mathbf{u}_D^\alpha$  are imposed on the boundaries  $\Gamma_D^\alpha$  whereas some surface forces  $\mathbf{F}^\alpha$  are applied on  $\Gamma_N^\alpha$ . For the sake of simplicity, body forces are not considered. We choose the orientation of the contact zone  $\Gamma^c$  by setting:  $\mathbf{n}^c = \mathbf{n}^1$ , see Fig. 1.

We introduce, on the interface  $\Gamma^c$ , the functions  $\mathbf{w}^1$  and  $\mathbf{w}^2$  representing two displacement fields defined on each side of the interface and  $\mathbf{w}_c$  an interior displacement field. We also

**Fig. 1** Notations



define  $\mathbf{t}^1$  and  $\mathbf{t}^2$ , representing two fields of surface density forces (stresses transmitted to  $\Omega^1$  and  $\Omega^2$ ) and  $\mathbf{t}^c$  an interior field of surface density forces.

Let  $\mathbf{V}^\alpha$  denote the Sobolev spaces  $\mathbf{H}^1(\Omega^\alpha)$  and let us define the sets of admissible displacement fields defined on  $\Omega^\alpha$ , the trace of which, on the interface  $\Gamma^c$ , is equal to a given displacement  $\mathbf{u}_D^\alpha$ :

$$\mathbf{V}^\alpha(\mathbf{u}_D^\alpha) = \{ \mathbf{v} \in \mathbf{H}^1(\Omega^\alpha); \quad \mathbf{u} = \mathbf{u}_D^\alpha \text{ on } \Gamma_D^\alpha \}.$$

The associated vector spaces are then defined as

$$\mathbf{V}^\alpha(0) = \{ \mathbf{v} \in \mathbf{H}^1(\Omega^\alpha); \quad \mathbf{u} = 0 \text{ on } \Gamma_D^\alpha \}.$$

Let us introduce the n-uplets  $\mathbf{d} = (\mathbf{u}^1, \mathbf{u}^2, \mathbf{w}^1, \mathbf{w}^2, \mathbf{w}^c)$  and  $\mathbf{s} = (\boldsymbol{\sigma}^1, \boldsymbol{\sigma}^2, \mathbf{t}^1, \mathbf{t}^2, \mathbf{t}^c)$ . The problem of unilateral contact consists on finding  $(\mathbf{d}, \mathbf{s})$  such that  $(\mathbf{u}^\alpha, \mathbf{w}^\alpha, \mathbf{w}^c)$  satisfy the kinematic conditions (1),  $(\boldsymbol{\sigma}^\alpha, \mathbf{t}^\alpha, \mathbf{t}^c)$  satisfy the equilibrium equations (2),  $(\mathbf{u}^\alpha, \boldsymbol{\sigma}^\alpha)$  satisfy the elastic constitutive relation (3) with the stiffness or elasticity tensors  $\mathbf{K}^\alpha$  and the strain tensor  $\boldsymbol{\varepsilon}(\mathbf{u})$ ,  $(\mathbf{w}^c, \mathbf{t}^c)$  satisfy the contact constitutive relation (4). For  $\alpha = 1, 2$ :

$$\left. \begin{aligned} \mathbf{u}^\alpha &\in \mathbf{V}^\alpha(\mathbf{u}_D^\alpha), \\ \mathbf{u}^\alpha &= \mathbf{w}^\alpha, \\ \mathbf{w}^c &= \mathbf{w}^1 - \mathbf{w}^2 \end{aligned} \right\} \text{ on } \Gamma^c. \quad (1)$$

$$\forall \mathbf{v} \in \mathbf{V}^\alpha(0), - \int_{\Omega^\alpha} \boldsymbol{\sigma}^\alpha \boldsymbol{\varepsilon}(\mathbf{v}) dV + \int_{\Gamma_N^\alpha} \mathbf{F}^\alpha \mathbf{v} dS + \int_{\Gamma^c} \mathbf{t}^\alpha \mathbf{v} dS = 0, \quad (2)$$

$$\mathbf{t}^c - \mathbf{t}^1 = 0 \quad \text{and} \quad \mathbf{t}^c + \mathbf{t}^2 = 0 \text{ on } \Gamma^c.$$

$$\boldsymbol{\sigma}^\alpha = \mathbf{K}^\alpha \boldsymbol{\varepsilon}(\mathbf{u}^\alpha) \text{ in } \Omega^\alpha. \quad (3)$$

$$\phi(-\mathbf{w}^c) + \phi^*(\mathbf{t}^c) + \mathbf{t}^c \cdot \mathbf{w}^c = 0 \text{ on } \Gamma^c, \quad (4)$$

where for any vector  $\mathbf{v}$ , the normal and the tangential components are defined according to  $v_n = \mathbf{v} \cdot \mathbf{n}^c$  and  $\mathbf{v}_t = \mathbf{v} - v_n \mathbf{n}^c$  and the convex potentials  $\phi$  and  $\phi^*$  are defined by

$$\phi(\mathbf{v}) = \begin{cases} 0 & \text{if } v_n \geq 0 \\ +\infty & \text{otherwise} \end{cases} \quad \text{and} \quad \phi^*(\mathbf{t}) = \begin{cases} 0 & \text{if } t_n \leq 0 \quad \text{and} \quad \mathbf{t}_t = 0 \\ +\infty & \text{otherwise.} \end{cases} \quad (5)$$

Moreover, for any pair  $(\mathbf{w}^c, \mathbf{t}^c)$  defined on  $\Gamma^c$ , the Legendre–Fenchel inequality, see [20], leads to

$$\phi(-\mathbf{w}^c) + \phi^*(\mathbf{t}^c) + \mathbf{t}^c \cdot \mathbf{w}^c \geq 0. \quad (6)$$

*Remark 1* Following [20], the relation defined by Eq. (4) is equivalent to the Coulomb's constitutive law (7) in a frictionless case:

$$w_n^c \leq 0, \quad t_n^c \leq 0, \quad t_n^c w_n^c = 0 \quad \text{and} \quad \mathbf{t}_t^c = 0 \text{ on } \Gamma^c, \quad (7)$$

### 3 Domain Decomposition Algorithm

In this section, we recall the Neumann–Neumann Domain Decomposition (NNDD) algorithm used to solve the unilateral contact problem defined by Eqs. (1)–(4). Given a non-negative parameter  $\theta$  and an initial arbitrary normal displacement  $\lambda_1$  belonging to Sobolev space  $H^{1/2}(\Gamma^c)$ , we define two sequences of displacements  $\mathbf{u}_p^\alpha$  on each solid  $\Omega^\alpha$ ,  $\alpha = 1, 2$ . Each iteration  $p$  of the NNDD algorithm is divided in two successive steps in which the problems can be independently solved.

As in the NNDD algorithm some displacement fields  $\lambda$  are imposed on the contact  $\Gamma^c$ , we define the corresponding displacements spaces

$$\begin{aligned}\mathcal{V}^\alpha(\lambda) &= \{ \mathbf{u} \in \mathbf{V}^\alpha(\mathbf{u}_D^\alpha) \text{ and } \mathbf{u} \cdot \mathbf{n}^c = \lambda \text{ on } \Gamma^c \}, \\ \mathcal{V}_0^\alpha &= \{ \mathbf{u} \in \mathbf{V}^\alpha(0) \text{ and } \mathbf{u} \cdot \mathbf{n}^c = 0 \text{ on } \Gamma^c \}.\end{aligned}$$

– Step 1 Two independent elasticity problems are solved on  $\Omega_1$  and  $\Omega_2$ :

1. In  $\Omega^1$ , the variational problem writes: Find  $(\mathbf{u}_p^1, \boldsymbol{\sigma}_p^1)$  defined on  $\Omega^1$  and  $(\mathbf{w}_p^1, \mathbf{t}_p^1)$  defined on  $\Gamma^c$  such that

$$\mathbf{u}_p^1 = \mathbf{u}_D^1 \text{ on } \Gamma_D^1, \quad \mathbf{u}_p^1 - \mathbf{w}_p^1 = 0 \quad \text{and} \quad \mathbf{w}_p^1 \mathbf{n}^1 = \lambda_p \text{ on } \Gamma^c, \quad (8)$$

$$\forall \mathbf{v} \in \mathcal{V}_0^1, \quad - \int_{\Omega^1} \boldsymbol{\sigma}_p^1 : \boldsymbol{\varepsilon}(\mathbf{v}) dV + \int_{\Gamma_N^1} \mathbf{F}^1 \mathbf{v} dS = 0, \quad (9)$$

$$\mathbf{t}_p^1 = \boldsymbol{\sigma}_p^1 \mathbf{n}^1 \text{ on } \Gamma^c,$$

$$\boldsymbol{\sigma}_p^1 = \mathbf{K}^1 \boldsymbol{\varepsilon}(\mathbf{u}_p^1) \text{ in } \Omega^1. \quad (10)$$

2. In  $\Omega^2$ , with the given  $\lambda_p$  normal displacement defined on  $\Gamma^c$ , we solve the following variational problem corresponding to a unilateral frictionless contact problem on  $\Gamma^c$ . Find  $(\mathbf{u}_p^2, \boldsymbol{\sigma}_p^2)$  defined on  $\Omega^2$  and  $(\mathbf{w}_p^2, \mathbf{t}_p^2)$  defined on  $\Gamma^c$  such that

$$\mathbf{u}_p^2 = \mathbf{u}_D^2 \text{ on } \Gamma_D^2, \quad \mathbf{u}_p^2 - \mathbf{w}_p^2 = 0 \quad \text{and} \quad \mathbf{w}_p^2 = \lambda_p \mathbf{n}^1 - \mathbf{w}_p^2 \text{ on } \Gamma^c, \quad (11)$$

$$\forall \mathbf{v} \in \mathcal{V}_0^2, \quad - \int_{\Omega^2} \boldsymbol{\sigma}_p^2 : \boldsymbol{\varepsilon}(\mathbf{v}) dV + \int_{\Gamma_N^2} \mathbf{F}^2 \mathbf{v} dS + \int_{\Gamma^c} \mathbf{t}_p^2 \mathbf{v} dS = 0, \quad (12)$$

$$\mathbf{t}_p^c + \mathbf{t}_p^2 = 0 \text{ on } \Gamma^c,$$

$$\boldsymbol{\sigma}_p^2 = \mathbf{K}^2 \boldsymbol{\varepsilon}(\mathbf{u}_p^2) \text{ in } \Omega^2, \quad (13)$$

$$\phi(-\mathbf{w}_p^c) + \phi^*(\mathbf{t}_p^c) + \mathbf{t}_p^c \cdot \mathbf{w}_p^c = 0 \text{ on } \Gamma^c. \quad (14)$$

– Step 2 With  $\mathbf{t}_p^1$  and  $\mathbf{t}_p^2$  obtained from Step 1, we solve two independent “Neumann type” problems:

In  $\Omega^1$ , we solve

$$\begin{cases} \text{Find } \mathbf{w}^1 \in \mathbf{V}^1(0) \text{ such that} \\ \int_{\Omega^1} \mathbf{K}^1 \boldsymbol{\varepsilon}(\mathbf{w}^1) : \boldsymbol{\varepsilon}(\mathbf{v}) dV = - \int_{\Gamma^c} \frac{1}{2} (\mathbf{t}_p^1 + \mathbf{t}_p^2) \cdot (\mathbf{v}) \quad \forall \mathbf{v} \in \mathbf{V}^1(0). \end{cases} \quad (15)$$

In  $\Omega^2$ , we solve

$$\begin{cases} \text{Find } \mathbf{w}^2 \in \mathbf{V}^2(0) \text{ such that} \\ \int_{\Omega^2} \mathbf{K}^2 \boldsymbol{\varepsilon}(\mathbf{w}^2) : \boldsymbol{\varepsilon}(\mathbf{v}) dV = \int_{\Gamma^c} \frac{1}{2} (\mathbf{t}_p^1 + \mathbf{t}_p^2) \cdot (\mathbf{v}) \quad \forall \mathbf{v} \in \mathbf{V}^2(0). \end{cases} \quad (16)$$

Let  $\varepsilon_\tau$  be the precision of the algorithm,

$$\varepsilon_\tau = \|(\mathbf{w}^1 - \mathbf{w}^2) \cdot \mathbf{n}\|_{H^{1/2}(\Gamma^c)}$$

we have the alternative:

1. If  $\varepsilon_\tau$  is small enough, the algorithm stops.

2. Else, on  $\Gamma^c$ , the normal displacement  $\lambda_p$  is updated:

$$\lambda_{p+1} := \lambda_p + \theta(\mathbf{w}^1 - \mathbf{w}^2) \cdot \mathbf{n}$$

and we return to Step 1 for iteration  $p + 1$ .

At the end of each iteration this algorithm yields an approximate solution  $(\mathbf{d}_p, \mathbf{s}_p)$  of the contact problem (1)–(4), with  $\mathbf{d}_p = (\mathbf{u}_p^1, \mathbf{u}_p^2, \mathbf{w}_p^1, \mathbf{w}_p^2, \mathbf{w}_p^c)$  and  $\mathbf{s}_p = (\boldsymbol{\sigma}_p^1, \boldsymbol{\sigma}_p^2, \mathbf{t}_p^1, \mathbf{t}_p^2, \mathbf{t}_p^c)$ . The convergence is obtained when  $\lambda_{p+1} - \lambda_p \rightarrow 0$ , that is when  $(\mathbf{w}^1 - \mathbf{w}^2) \cdot \mathbf{n} \rightarrow 0$  on  $\Gamma^c$ .

**Proposition 1**  $(\mathbf{w}^1 - \mathbf{w}^2) \cdot \mathbf{n} = 0$  on  $\Gamma^c \implies (\mathbf{d}_p, \mathbf{s}_p) = (\mathbf{d}, \mathbf{s})$  the solution of the contact problem (1)–(4).

*Proof* Suppose  $(\mathbf{w}^1 - \mathbf{w}^2) \cdot \mathbf{n} = 0$  on  $\Gamma^c$ , replacing respectively  $\mathbf{w}^1$  and  $\mathbf{w}^2$  in (15) and (16), we obtain the following equalities:

$$\begin{aligned} \int_{\Omega^1} \mathbf{K}^2 \boldsymbol{\varepsilon}(\mathbf{w}^1) : \boldsymbol{\varepsilon}(\mathbf{w}^1) dV &= - \int_{\Gamma^c} \frac{1}{2} (\mathbf{t}_p^1 + \mathbf{t}_p^2) \cdot (\mathbf{w}^1) \\ \int_{\Omega^2} \mathbf{K}^2 \boldsymbol{\varepsilon}(\mathbf{w}^2) : \boldsymbol{\varepsilon}(\mathbf{w}^2) dV &= \int_{\Gamma^c} \frac{1}{2} (\mathbf{t}_p^1 + \mathbf{t}_p^2) \cdot (\mathbf{w}^2) \end{aligned}$$

Summing up, we obtain, since the stress vectors  $\mathbf{t}_p^1$  and  $\mathbf{t}_p^2$  have no tangential component:

$$\int_{\Omega^1} \mathbf{K}^2 \boldsymbol{\varepsilon}(\mathbf{w}^1) : \boldsymbol{\varepsilon}(\mathbf{w}^1) dV + \int_{\Omega^2} \mathbf{K}^2 \boldsymbol{\varepsilon}(\mathbf{w}^2) : \boldsymbol{\varepsilon}(\mathbf{w}^2) dV = 0.$$

As the quadratic forms are positive, this means that  $\mathbf{w}^1 \equiv 0$  and  $\mathbf{w}^2 \equiv 0$ , and thus,  $\mathbf{t}_p^1 + \mathbf{t}_p^2 = 0$  on  $\Gamma^c$ . In other words, at this point, the solutions  $\mathbf{u}_p^\alpha$  from the NNDD algorithm satisfy the unilateral contact problem (1)–(4).

As, in the NNDD algorithm, the solution of the unilateral contact problem (1)–(4) is obtained when the sequence  $\lambda_p$  is convergent. The convergence of the NNDD algorithm can be proved by showing that the mapping  $T_\theta$  for any  $\lambda \in H^{1/2}(\Gamma^c)$  and its associated respective solutions  $\mathbf{w}^1$  and  $\mathbf{w}^2$  of (15) and (16),

$$T_\theta(\lambda) = \lambda + \theta(\mathbf{w}^1 - \mathbf{w}^2) \cdot \mathbf{n}$$

is a contraction in  $H^{1/2}(\Gamma^c)$  for any  $\theta$  small enough, see [18, 19]:

**Proposition 2** *There is a  $\theta_0 > 0$  such that for any  $0 < \theta \leq \theta_0$ , the NNDD algorithm for unilateral frictionless contact converges.*

#### 4 Finite Element Approximation

At each step  $p$ , approximate solution of problems (8)–(10), (11)–(14) and (15)–(16) are computed using a classical FE method. The problem (8)–(10) and the problems (15)–(16) lead to standard linear variational problems and the problem (11)–(13) is solved as a variational problem with affine inequality constraint.

Let  $\mathbf{V}_h^\alpha$  be some finite element spaces respectively discretizing the Sobolev spaces  $\mathbf{V}^\alpha = \mathbf{H}^1(\Omega^\alpha)$ . We define

$$\begin{aligned}\mathbf{V}_h^\alpha(\mathbf{u}_D^\alpha) &= \mathbf{V}^\alpha(\mathbf{u}_D^\alpha) \cap \mathbf{V}_h^\alpha \\ \mathbf{V}_h^\alpha(0) &= \mathbf{V}^\alpha(0) \cap \mathbf{V}_h^\alpha, \\ \mathcal{V}_h^1(\lambda) &= \mathcal{V}^1(\lambda) \cap \mathbf{V}_h^1, \\ \mathcal{V}_h^1(0) &= \mathcal{V}^1(0) \cap \mathbf{V}_h^1,\end{aligned}$$

and

$$\mathcal{K}_h^2(\lambda) = \{\mathbf{v} \in \mathbf{V}_h^2(\mathbf{u}_D^2) \text{ and } \mathbf{v} \cdot \mathbf{n}^c \geq \lambda \text{ on } \Gamma^c\}.$$

The approximate solutions of (8)–(10), (11)–(14), (15) and (16) are respectively given by

$$\left\{ \begin{array}{l} \text{Find } \mathbf{u}_{p,h}^1 \in \mathcal{V}_h^\alpha(\lambda_p) \text{ such that} \\ \int_{\Omega^1} \mathbf{K}^1 \boldsymbol{\varepsilon}(\mathbf{u}_{p,h}^1) \boldsymbol{\varepsilon}(\mathbf{v}) dV = \int_{\Gamma_N^1} \mathbf{F}^1 \mathbf{v} dS \quad \forall \mathbf{v} \in \mathcal{V}_h^1(0), \end{array} \right. \quad (17)$$

$$\left\{ \begin{array}{l} \text{Find } \mathbf{u}_{p,h}^2 \in \mathcal{K}_h^\alpha(\lambda_p) \text{ such that} \\ \int_{\Omega^2} \mathbf{K}^2 \boldsymbol{\varepsilon}(\mathbf{u}_{p,h}^2) \boldsymbol{\varepsilon}(\mathbf{v}) dV \geq \int_{\Gamma_N^2} \mathbf{F}^2 \mathbf{v} dS \quad \forall \mathbf{v} \in \mathcal{K}_h^\alpha(\lambda_p), \end{array} \right. \quad (18)$$

$$\left\{ \begin{array}{l} \text{Find } \mathbf{w}_{p,h}^1 \in \mathbf{V}_h^\alpha(\mathbf{u}_D^1) \text{ such that} \\ \int_{\Omega^1} \mathbf{K}^1 \boldsymbol{\varepsilon}(\mathbf{w}_{p,h}^1) \boldsymbol{\varepsilon}(\mathbf{v}) dV = \int_{\Gamma^c} -\frac{1}{2}(\mathbf{t}_{p,h}^1 + \mathbf{t}_{p,h}^2) \cdot \mathbf{v} dS \quad \forall \mathbf{v} \in \mathbf{V}_h^1(0), \end{array} \right. \quad (19)$$

$$\left\{ \begin{array}{l} \text{Find } \mathbf{w}_{p,h}^2 \in \mathbf{V}_h^\alpha(\mathbf{u}_D^2) \text{ such that} \\ \int_{\Omega^2} \mathbf{K}^2 \boldsymbol{\varepsilon}(\mathbf{w}_{p,h}^2) \boldsymbol{\varepsilon}(\mathbf{v}) dV = \int_{\Gamma^c} \frac{1}{2}(\mathbf{t}_{p,h}^1 + \mathbf{t}_{p,h}^2) \cdot \mathbf{v} dS \quad \forall \mathbf{v} \in \mathbf{V}_h^2(0), \end{array} \right. \quad (20)$$

where  $\mathbf{t}_{p,h}^1$  in (19) and  $\mathbf{t}_{p,h}^2$  in (20) are derived from the fields  $u_{p,h}^1$  and  $u_{p,h}^2$  computed in Eqs. (17) and (18) by

$$\mathbf{t}_{p,h}^i = \sigma_{p,h}^i n^i \text{ on } \Gamma^i \quad \text{where } \sigma_{p,h}^i = \mathbf{K}^i \boldsymbol{\varepsilon}(\mathbf{u}_{p,h}^i) \quad \text{for } i = 1, 2$$

and

$$\mathbf{w}_{p,h}^c = \lambda_p \mathbf{n}^c - \mathbf{w}_{p,h}^2 \text{ on } \Gamma^c.$$

We shall denote

$$\mathbf{d}_{p,h} = (\mathbf{u}_{p,h}^1, \mathbf{w}_{p,h}^1, \mathbf{u}_{p,h}^2, \mathbf{w}_{p,h}^2, \mathbf{w}_{p,h}^c) \quad (21)$$

$$\mathbf{s}_{p,h} = (\sigma_{p,h}^1, \mathbf{t}_{p,h}^1, \sigma_{p,h}^2, \mathbf{t}_{p,h}^2, \mathbf{t}_{p,h}^c). \quad (22)$$

*Remark 2* For the sake of simplicity, the Finite Element formulations (17)–(20) are written here for matching meshes at the interface, however, the extension to non matching meshes is straightforward (see [8]).

## 5 Error Estimation

### 5.1 Error in the Constitutive Relation

To develop an error estimation for a contact problem we use a method based on the constitutive relation error [5]. We recall here the error measure proposed in [8] for a global unilateral contact problem. Let us consider an approximate solution of problem defined by Eqs. (1)–(4), denoted  $(\hat{\mathbf{d}}, \hat{\mathbf{s}})$ . The pair  $(\hat{\mathbf{d}}, \hat{\mathbf{s}})$  is said to be an *admissible* solution if  $(\hat{\mathbf{d}}, \hat{\mathbf{s}}) \in \mathcal{U}_{ad} \times \mathcal{S}_{ad}$  where

$$\begin{aligned} \mathcal{U}_{ad} &= \text{the set of the kinematically admissible fields} \\ &= \{\hat{\mathbf{d}} = (\hat{\mathbf{u}}^1, \hat{\mathbf{u}}^2, \hat{\mathbf{w}}^1, \hat{\mathbf{w}}^2, \hat{\mathbf{w}}^c) / \hat{\mathbf{d}} \text{ satisfies Eq. (1) and } \phi(-\hat{\mathbf{w}}^c) = 0\}, \end{aligned}$$

and

$$\begin{aligned} \mathcal{S}_{ad} &= \text{the set of the statically admissible fields} \\ &= \{\hat{\mathbf{s}} = (\hat{\boldsymbol{\sigma}}^1, \hat{\boldsymbol{\sigma}}^2, \hat{\mathbf{t}}^1, \hat{\mathbf{t}}^2, \hat{\mathbf{t}}^c) / \hat{\mathbf{s}} \text{ satisfies Eq. (2) and } \phi^*(\hat{\mathbf{t}}^c) = 0\}. \end{aligned}$$

The constitutive relation error on the pair  $(\hat{\mathbf{d}}, \hat{\mathbf{s}})$  is defined by

$$e_{CRE}(\hat{\mathbf{d}}, \hat{\mathbf{s}}) = \left[ \sum_{\alpha=1}^2 \|\hat{\boldsymbol{\sigma}}^\alpha - \mathbf{K}^\alpha \boldsymbol{\varepsilon}(\hat{\mathbf{u}}^\alpha)\|_{\boldsymbol{\sigma}, \Omega^\alpha}^2 + 2 \int_{\Gamma^c} \hat{\mathbf{t}}^c \hat{\mathbf{w}}^c dS \right]^{1/2}, \quad (23)$$

with

$$\|\hat{\boldsymbol{\sigma}}\|_{\boldsymbol{\sigma}, \Omega^\alpha}^2 = \int_{\Omega^\alpha} \hat{\boldsymbol{\sigma}} : (\mathbf{K}^\alpha)^{-1} \hat{\boldsymbol{\sigma}}.$$

Note that factor 2 before the integral of expression (23) will prove sufficient to obtain the upper bound property of Proposition 6.

*Remark 3* It should be noted that as  $\phi(-\hat{\mathbf{w}}^c) = 0$  and  $\phi^*(\hat{\mathbf{t}}^c) = 0$ , from (6), the quantity  $\hat{\mathbf{t}}^c \hat{\mathbf{w}}^c$  is greater than zero on  $\Gamma^c$ .

As an extension of the Prager–Synge theorem [21], it was shown in [8] that

$$e_{CRE}(\hat{\mathbf{d}}, \hat{\mathbf{s}}) \geq \left[ \sum_{\alpha=1}^2 \|\hat{\boldsymbol{\sigma}}^\alpha - \boldsymbol{\sigma}^\alpha\|_{\boldsymbol{\sigma}, \Omega^\alpha}^2 + \|\hat{\mathbf{u}}^\alpha - \mathbf{u}^\alpha\|_{\mathbf{u}, \Omega^\alpha}^2 \right]^{1/2}, \quad (24)$$

with

$$\|\hat{\mathbf{u}}\|_{\mathbf{u}, \Omega^\alpha}^2 = \int_{\Omega^\alpha} \mathbf{K}^\alpha \boldsymbol{\varepsilon}(\hat{\mathbf{u}}) : \boldsymbol{\varepsilon}(\hat{\mathbf{u}}).$$

### 5.2 An a Posteriori Error Estimator for a Discretized Neumann–Neumann Domain Decomposition Algorithm

When the formulation of the contact problem is obtained by a domain decomposition method the global error depends not only on the FE discretization error but also on the convergence of the iterative algorithm used (*i.e.* an algebraic error). Here, we develop an error measure based on the constitutive relation error for a unilateral contact problem solved by a Neumann–Neumann domain decomposition algorithm. Let us introduce new admissible sets defined at each iteration  $p$  of the NNDD algorithm by



$$\begin{aligned}
\mathcal{U}_{ad}^1(\lambda_p) &= \{\hat{\mathbf{d}}^1 = (\hat{\mathbf{u}}^1, \hat{\mathbf{w}}^1)/\hat{\mathbf{d}}^1 \text{ satisfies Eq. (8)}\}, \\
\mathcal{S}_{ad}^1 &= \{\hat{\mathbf{s}}^1 = (\hat{\boldsymbol{\sigma}}^1, \hat{\mathbf{t}}^1)/\hat{\mathbf{s}}^1 \text{ satisfies Eq. (9)}\}, \\
\mathcal{U}_{ad}^2(\lambda_p) &= \{\hat{\mathbf{d}}^2 = (\hat{\mathbf{u}}^2, \hat{\mathbf{w}}^2, \hat{\mathbf{w}}^c)/\hat{\mathbf{d}}^2 \text{ satisfies Eq. (11) and } \phi(-\hat{\mathbf{w}}^c) = 0\}, \\
\mathcal{S}_{ad}^2(\lambda_p) &= \{\hat{\mathbf{s}}^2 = (\hat{\boldsymbol{\sigma}}^2, \hat{\mathbf{t}}^2, \hat{\mathbf{t}}^c)/\hat{\mathbf{s}}^2 \text{ satisfies Eq. (12) and } \phi^*(\hat{\mathbf{t}}^c) = 0\}.
\end{aligned}$$

**Proposition 3** *The pair  $(\hat{\mathbf{d}}_p^1, \hat{\mathbf{s}}_p^1) \in \mathcal{U}_{ad}^1(\lambda_p) \times \mathcal{S}_{ad}^1$  is the solution of problem (8)–(10) if*

$$e_{CRE}^1(\hat{\mathbf{d}}_p^1, \hat{\mathbf{s}}_p^1) = \left[ \|\hat{\boldsymbol{\sigma}}_p^1 - \mathbf{K}^1 \boldsymbol{\varepsilon}(\hat{\mathbf{u}}_p^1)\|_{\boldsymbol{\sigma}, \Omega^1}^2 \right]^{1/2} = 0. \quad (25)$$

*Proof* Since  $(\hat{\mathbf{d}}_p^1, \hat{\mathbf{s}}_p^1)$  belongs to  $\mathcal{U}_{ad}^1(\lambda_p) \times \mathcal{S}_{ad}^1(\lambda_p)$ , Eqs. (8) and (9) are satisfied. Eq. (10) then follows from the condition (25).

**Proposition 4** *The pair  $(\hat{\mathbf{d}}_p^2, \hat{\mathbf{s}}_p^2) \in \mathcal{U}_{ad}^2(\lambda_p) \times \mathcal{S}_{ad}^2(\lambda_p)$  is the solution of problem (11)–(14) if*

$$e_{CRE}^2(\hat{\mathbf{d}}_p^2, \hat{\mathbf{s}}_p^2) = \left[ \|\hat{\boldsymbol{\sigma}}_p^2 - \mathbf{K}^2 \boldsymbol{\varepsilon}(\hat{\mathbf{u}}_p^2)\|_{\boldsymbol{\sigma}, \Omega^2}^2 + 2 \int_{\Gamma^c} \hat{\mathbf{t}}_p^c \hat{\mathbf{w}}_p^c dS \right]^{1/2} = 0. \quad (26)$$

*Proof* Since  $(\hat{\mathbf{d}}_p^2, \hat{\mathbf{s}}_p^2)$  belongs to  $\mathcal{U}_{ad}^2(\lambda_p) \times \mathcal{S}_{ad}^2(\lambda_p)$ , Eqs. (11) and (12) are satisfied. Moreover as  $\hat{\mathbf{d}}_p^2 \in \mathcal{U}_{ad}^2(\lambda_p)$  and  $\hat{\mathbf{s}}_p^2 \in \mathcal{S}_{ad}^2(\lambda_p)$ , we have  $\hat{\mathbf{w}}_p^c \geq 0$  and  $\hat{\mathbf{t}}_p^c \geq 0$  on  $\Gamma^c$  and, see Remark 3:

$$\int_{\Gamma^c} \hat{\mathbf{t}}_p^c \hat{\mathbf{w}}_p^c dS \geq 0. \quad (27)$$

It follows then from (26) that  $\hat{\boldsymbol{\sigma}}_p^2 - \mathbf{K}^2 \boldsymbol{\varepsilon}(\hat{\mathbf{u}}_p^2) = 0$  on  $\Omega^2$ , hence that  $(\hat{\mathbf{d}}_p^2, \hat{\mathbf{s}}_p^2)$  satisfy Eq. (13), and

$$\hat{\mathbf{t}}_p^c \cdot \hat{\mathbf{w}}_p^c = 0 \text{ on } \Gamma^c. \quad (28)$$

Morover, as  $\hat{\mathbf{d}}_p^2 \in \mathcal{U}_{ad}^2(\lambda_p)$  and  $\hat{\mathbf{s}}_p^2 \in \mathcal{S}_{ad}^2(\lambda_p)$ , we have  $\phi(-\hat{\mathbf{w}}^c) = 0$  and  $\phi(\hat{\mathbf{t}}_p^c) = 0$ , hence Eq. (14) is satisfied.

*Remark 4* We emphasize that the pair  $(\hat{\mathbf{d}}_p = (\hat{\mathbf{d}}_p^1, \hat{\mathbf{d}}_p^2), \hat{\mathbf{s}}_p = (\hat{\mathbf{s}}_p^1, \hat{\mathbf{s}}_p^2))$  is not, a priori, an admissible solution for the unilateral contact problem (i.e.  $\notin \mathcal{U}_{ad} \times \mathcal{S}_{ad}$ ) because the equilibrium equation (2) is not necessarily satisfied since  $\hat{\mathbf{t}}_p^c - \hat{\mathbf{t}}_p^1 = 0$  has not been imposed.

We define then an error estimator for the problem defined by Eqs. (8)–(14), with

$$e_{CRE}(\hat{\mathbf{d}}_p, \hat{\mathbf{s}}_p) = \left[ \left( e_{CRE}^1(\hat{\mathbf{d}}_p^1, \hat{\mathbf{s}}_p^1) \right)^2 + \left( e_{CRE}^2(\hat{\mathbf{d}}_p^2, \hat{\mathbf{s}}_p^2) \right)^2 \right]^{1/2}. \quad (29)$$

Following from Proposition 3 and 4, we have

**Proposition 5** *The error estimator  $e_{CRE}(\hat{\mathbf{d}}_p, \hat{\mathbf{s}}_p)$  defined in (29), quantifies the error due to the finite element discretization at each step of the algorithm.*

$$e_{CRE}(\hat{\mathbf{d}}_p, \hat{\mathbf{s}}_p) = 0 \Leftrightarrow (\hat{\mathbf{d}}_p^1, \hat{\mathbf{s}}_p^1, \hat{\mathbf{d}}_p^2, \hat{\mathbf{s}}_p^2) \text{ is the exact solution of (8)–(14) for a fixed } \lambda_p.$$

Furthermore, we have,

**Proposition 6** *The error estimator (29) is an upper bound for the exact error of (8)–(14) for a fixed  $\lambda_p$ .*

*Proof* For a given  $\lambda_p$ , let us denote by  $(\mathbf{d}_p^1, \mathbf{s}_p^1)$ , resp.  $(\mathbf{d}_p^2, \mathbf{s}_p^2)$ , the exact solution of problem (8)–(10), resp. problem (11)–(14), from step 1 of NNDD algorithm.

As (8)–(10) defines a linear elastic problem we can use the Prager–Synge theorem [21] to obtain

$$(e_{CRE}^1)^2 = \|\hat{\boldsymbol{\sigma}}_p^1 - \mathbf{K}\boldsymbol{\varepsilon}(\hat{\mathbf{u}}_p^1)\|_{\boldsymbol{\sigma}, \Omega^1}^2 = \|\hat{\boldsymbol{\sigma}}_p^1 - \boldsymbol{\sigma}_p^1\|_{\boldsymbol{\sigma}, \Omega^1}^2 + \|\hat{\mathbf{u}}_p^1 - \mathbf{u}_p^1\|_{\mathbf{u}, \Omega^1}^2. \quad (30)$$

Considering (11)–(14), the error estimator writes

$$\begin{aligned} (e_{CRE}^2)^2 &= \|\hat{\boldsymbol{\sigma}}_p^2 - \mathbf{K}^2\boldsymbol{\varepsilon}(\hat{\mathbf{u}}_p^2)\|_{\boldsymbol{\sigma}, \Omega^2}^2 + 2 \int_{\Gamma^c} \hat{\mathbf{t}}_p^2 \hat{\mathbf{w}}_p^2 \\ &= \|\hat{\boldsymbol{\sigma}}_p^2 - \boldsymbol{\sigma}_p^2 + \mathbf{K}^2\boldsymbol{\varepsilon}(\mathbf{u}_p^2) - \mathbf{K}^2\boldsymbol{\varepsilon}(\hat{\mathbf{u}}_p^2)\|_{\boldsymbol{\sigma}, \Omega^2}^2 + 2 \int_{\Gamma^c} \hat{\mathbf{t}}_p^2 \hat{\mathbf{w}}_p^2 dS \\ &= \|\hat{\boldsymbol{\sigma}}_p^2 - \boldsymbol{\sigma}_p^2\|_{\boldsymbol{\sigma}, \Omega^2}^2 + \|\hat{\mathbf{u}}_p^2 - \mathbf{u}_p^2\|_{\mathbf{u}, \Omega^2}^2 + C \end{aligned}$$

with

$$C = 2 \int_{\Omega^2} (\hat{\boldsymbol{\sigma}}_p^2 - \boldsymbol{\sigma}_p^2) : \boldsymbol{\varepsilon}(\mathbf{u}_p^2 - \hat{\mathbf{u}}_p^2) dV + 2 \int_{\Gamma^c} \hat{\mathbf{t}}_p^2 \hat{\mathbf{w}}_p^2 dS. \quad (31)$$

In other words, we have

$$\begin{aligned} (e_{CRE}^1)^2 + (e_{CRE}^2)^2 &= \|\hat{\boldsymbol{\sigma}}_p^1 - \boldsymbol{\sigma}_p^1\|_{\boldsymbol{\sigma}, \Omega^1}^2 + \|\hat{\mathbf{u}}_p^1 - \mathbf{u}_p^1\|_{\mathbf{u}, \Omega^1}^2 \\ &\quad + \|\hat{\boldsymbol{\sigma}}_p^2 - \boldsymbol{\sigma}_p^2\|_{\boldsymbol{\sigma}, \Omega^2}^2 + \|\hat{\mathbf{u}}_p^2 - \mathbf{u}_p^2\|_{\mathbf{u}, \Omega^2}^2 + C. \end{aligned}$$

Thus, we only need to show that  $C \geq 0$ :

As  $\mathbf{u}_p^2 - \hat{\mathbf{u}}_p^2 \in \mathcal{V}_0^2$  and thanks to Eq. (12) we have

$$\begin{aligned} \int_{\Omega^2} \boldsymbol{\sigma}_p^2 : \boldsymbol{\varepsilon}(\mathbf{u}_p^2 - \hat{\mathbf{u}}_p^2) dV &= \int_{\Gamma_N^2} \mathbf{F}^2(\mathbf{u}_p^2 - \hat{\mathbf{u}}_p^2) dS + \int_{\Gamma^c} \mathbf{t}_p^2(\mathbf{u}_p^2 - \hat{\mathbf{u}}_p^2) dS \\ \int_{\Omega^2} \hat{\boldsymbol{\sigma}}_p^2 : \boldsymbol{\varepsilon}(\mathbf{u}_p^2 - \hat{\mathbf{u}}_p^2) dV &= \int_{\Gamma_N^2} \mathbf{F}^2(\mathbf{u}_p^2 - \hat{\mathbf{u}}_p^2) dS + \int_{\Gamma^c} \hat{\mathbf{t}}_p^2(\mathbf{u}_p^2 - \hat{\mathbf{u}}_p^2) dS \end{aligned}$$

therefore by subtraction, we obtain

$$\int_{\Omega^2} (\hat{\boldsymbol{\sigma}}_p^2 - \boldsymbol{\sigma}_p^2) : \boldsymbol{\varepsilon}(\mathbf{u}_p^2 - \hat{\mathbf{u}}_p^2) dV = \int_{\Gamma^c} (\hat{\mathbf{t}}_p^2 - \mathbf{t}_p^2)(\mathbf{w}_p^2 - \hat{\mathbf{w}}_p^2) dS.$$

As  $\mathbf{u}_p^2$  and  $\hat{\mathbf{u}}_p^2$  belong to  $\mathcal{V}^2(\lambda_p)$  their restriction to  $\Gamma^c$  are respectively equal to  $\mathbf{w}_p^2$  and  $\hat{\mathbf{w}}_p^2$ , so that  $C$  writes

$$\begin{aligned} C &= 2 \int_{\Gamma^c} (\hat{\mathbf{t}}_p^2 - \mathbf{t}_p^2)(\mathbf{w}_p^2 - \hat{\mathbf{w}}_p^2) dS + 2 \int_{\Gamma^c} \hat{\mathbf{t}}_p^2 \hat{\mathbf{w}}_p^2 \\ &= 2 \int_{\Gamma^c} (\hat{\mathbf{t}}_p^2 \mathbf{w}_p^2 + \mathbf{t}_p^2 \hat{\mathbf{w}}_p^2 - \mathbf{t}_p^2 \mathbf{w}_p^2) dS \\ &= 2 \int_{\Gamma^c} (\hat{\mathbf{t}}_p^2 \mathbf{w}_p^2 + \mathbf{t}_p^2 \hat{\mathbf{w}}_p^2) dS \end{aligned}$$

Finally, remarking that  $\phi^*(\hat{\mathbf{t}}_p^2) = 0$  and  $\phi(\mathbf{w}_p^2) = 0$ , as well as  $\phi^*(\mathbf{t}_p^2) = 0$  and  $\phi(\hat{\mathbf{w}}_p^2) = 0$ , see (6), leads to  $C \geq 0$  which concludes the proof.

In order to obtain a global error estimator for the contact problem, we define an admissible solution for the unilateral contact problem ( $\hat{\mathbf{d}}_p = (\hat{\mathbf{d}}_p^1, \hat{\mathbf{d}}_p^2)$ ,  $\hat{\mathbf{s}}_p = (\hat{\mathbf{s}}_p^1, \hat{\mathbf{s}}_p^2)$ ) that is

$$\begin{aligned} (\hat{\mathbf{d}}_p^1, \hat{\mathbf{s}}_p^1) &\in \mathcal{U}_{ad}^1(\lambda_p) \times \mathcal{S}_{ad}^1, \\ (\hat{\mathbf{d}}_p^2, \hat{\mathbf{s}}_p^2) &\in \mathcal{U}_{ad}^2(\lambda_p) \times \mathcal{S}_{ad}^2(\lambda_p), \\ \hat{\mathbf{t}}_p^c - \hat{\mathbf{t}}_p^1 &= 0. \end{aligned}$$

The global error estimator for the contact problem is then defined by

$$\eta^{glo} = e_{CRE}(\hat{\mathbf{d}}_p, \hat{\mathbf{s}}_p) = \left[ \left( e_{CRE}^1(\hat{\mathbf{d}}_p^1, \hat{\mathbf{s}}_p^1) \right)^2 + \left( e_{CRE}^2(\hat{\mathbf{d}}_p^2, \hat{\mathbf{s}}_p^2) \right)^2 \right]^{\frac{1}{2}}. \quad (32)$$

We have the following property:

**Proposition 7** *Let  $(\hat{\mathbf{d}}_p, \hat{\mathbf{s}}_p)$  be an admissible solution for the unilateral contact problem, it is the exact solution of global unilateral contact problem defined by (1)–(4) if and only if*

$$e_{CRE}(\hat{\mathbf{d}}_p, \hat{\mathbf{s}}_p) = 0.$$

*Proof* If  $(\hat{\mathbf{d}}_p, \hat{\mathbf{s}}_p)$  is the exact solution of the global unilateral contact problem, then it satisfy Eqs. (3)–(4), then  $e_{CRE}(\hat{\mathbf{d}}_p, \hat{\mathbf{s}}_p) = 0$  follows immediately.

If  $e_{CRE}(\hat{\mathbf{d}}_p, \hat{\mathbf{s}}_p) = 0$ , according to Propositions 3 and 4, as  $(\hat{\mathbf{d}}_p^1, \hat{\mathbf{s}}_p^1) \in \mathcal{U}_{ad}^1(\lambda_p) \times \mathcal{S}_{ad}^1$  and  $(\hat{\mathbf{d}}_p^2, \hat{\mathbf{s}}_p^2) \in \mathcal{U}_{ad}^2(\lambda_p) \times \mathcal{S}_{ad}^2(\lambda_p)$  it follows that  $(\hat{\mathbf{d}}_p, \hat{\mathbf{s}}_p)$  satisfies Eqs. (8)–(14). From Eq. (12) it follows that  $\hat{\mathbf{t}}_p^c + \hat{\mathbf{t}}_p^2 = 0$ , which combined with  $\hat{\mathbf{t}}_p^c - \hat{\mathbf{t}}_p^1 = 0$  leads to  $\hat{\mathbf{t}}_p^1 + \hat{\mathbf{t}}_p^2 = 0$ . Then, from Proposition 1,  $(\hat{\mathbf{d}}_p, \hat{\mathbf{s}}_p)$ , is the exact solution of the global unilateral contact problem.

*Remark 5* The admissible displacement fields are easily recovered, since the finite element fields satisfy the kinematic constraints and  $\mathbf{w}_{p,h}^c(x_i) \geq 0$ , where  $x_i$  denote the nodes of the FEM on the contact zone  $\Gamma^c$ .

$$\hat{\mathbf{d}}_p^1 = (\mathbf{u}_{p,h}^1, \mathbf{w}_{p,h}^1) \quad \text{and} \quad \hat{\mathbf{d}}_p^2 = (\mathbf{u}_{p,h}^2, \mathbf{w}_{p,h}^2, \mathbf{w}_{p,h}^c).$$

However, the stress fields and the traction forces  $\mathbf{s}_{p,h}$ , see (22), computed by the algorithm do not satisfy the equilibrium equations. The pair  $(\hat{\mathbf{s}}_p^1, \hat{\mathbf{s}}_p^2)$  is recovered from the finite element solution and the data in 3 steps

- The first step, consists in recovering admissible traction fields  $(\hat{\mathbf{t}}^1, \hat{\mathbf{t}}^2, \hat{\mathbf{t}}^c)$ . We built a traction  $\hat{\mathbf{t}}^c$  such that  $\phi^*(\hat{\mathbf{t}}^c) = 0$  and which minimizes in the least square sense  $J(\hat{\mathbf{t}}^c)$

$$J(\hat{\mathbf{t}}^c) = \int_{\Gamma^c} \left( \hat{\mathbf{t}}^c - \frac{1}{2} (\mathbf{t}_{h,p}^1 - \mathbf{t}_{h,p}^2) \right)^2 dS.$$

- The second step, consists in recovering stress fields  $\tilde{\boldsymbol{\sigma}}_{h,p}^\alpha$  that satisfy the FE-equilibrium equations on each solid  $\Omega^\alpha$ . Let  $\tilde{\mathbf{u}}_{h,p}^\alpha \in \mathcal{V}_h^\alpha$  such that  $\tilde{\boldsymbol{\sigma}}_{h,p}^\alpha = \mathbf{K}^\alpha \boldsymbol{\varepsilon}(\tilde{\mathbf{u}}_{h,p}^\alpha)$  and

$$\forall \mathbf{v} \in \mathcal{V}_{h,0}^\alpha, \quad - \int_{\Omega^\alpha} \mathbf{K}^\alpha \boldsymbol{\varepsilon}(\tilde{\mathbf{u}}_{h,p}^\alpha) : \boldsymbol{\varepsilon}(\mathbf{v}) dV + \int_{\Gamma_N} \mathbf{F}^\alpha \mathbf{v} dS + \int_{\Gamma^c} \hat{\mathbf{t}}^\alpha \mathbf{v} dS = 0.$$

- Finally, the recovery of equilibrated stress fields  $\hat{\boldsymbol{\sigma}}^\alpha$  from  $\tilde{\boldsymbol{\sigma}}_{h,p}^\alpha = \mathbf{K}^\alpha \boldsymbol{\varepsilon}(\tilde{\mathbf{u}}_{h,p}^\alpha)$ ,  $\mathbf{F}^\alpha$  and  $\hat{\mathbf{t}}^\alpha$  in each subdomain  $\Omega^\alpha$  is the most technical point. This step is performed with a traction-free recovery technique developed in [22].

Let us define the following error between the exact and approximate solution of the contact problem

$$e_{h,p} = \left[ \sum_{\alpha=1}^2 \|\mathbf{u}^\alpha - \mathbf{u}_{h,p}^\alpha\|_{\mathbf{u},\Omega^\alpha}^2 \right]^{1/2} \quad (33)$$

Repeating the proof of Proposition 6 with the exact solution of the unilateral contact problem leads to

**Proposition 8** *The global error estimator  $e_{CRE}(\hat{\mathbf{d}}_p, \hat{\mathbf{s}}_p)$  is an upper bound of the error  $e_{h,p}$ .*

### 5.3 Error Indicators for the NNDD Algorithm and for the FE Discretization

Following the method proposed in [23–25], we propose here two error indicators that allow us to estimate separately the part of the error due to the FE discretization from the part due to the NNDD algorithm. The discretization error is defined as the limit of the global error when the convergence criterion of the iterative algorithm tends to zero. The NNDD algorithm error is defined as the limit of the global error as the mesh size  $h$  tends to zero.

#### 5.3.1 Error Indicator for the FE Discretization

To define FE discretization error indicator  $\eta^{FE}$ , let us consider the reference problem defined by the step  $p$  of the NNDD algorithm: Find  $\mathbf{d}_p = (\mathbf{u}_p^1, \mathbf{w}_p^1, \mathbf{u}_p^2, \mathbf{w}_p^2, \mathbf{w}_p^c)$  and  $\mathbf{s}_p = (\boldsymbol{\sigma}_p^1, \mathbf{t}_p^1, \boldsymbol{\sigma}_p^2, \mathbf{t}_p^2, \mathbf{t}_p^c)$  that satisfy equations (8)–(14). The only approximation introduced between  $(\mathbf{d}_p, \mathbf{s}_p)$  and the finite element solution  $(\mathbf{d}_{p,h}, \mathbf{s}_{p,h})$  is the FE discretization. We have shown in Sect. 5.2 that the error in the constitutive relation  $e_{CRE}(\hat{\mathbf{d}}_p, \hat{\mathbf{s}}_p)$  defined in Eq. (29) is an error estimator for this reference problem. The quantity  $e_{CRE}(\hat{\mathbf{d}}_p, \hat{\mathbf{s}}_p)$  is used to define a FE discretization error indicator for the unilateral contact problem

$$\eta^{FE} = e_{CRE}(\hat{\mathbf{d}}_p, \hat{\mathbf{s}}_p). \quad (34)$$

*Remark 6* As shown on Sect. 5.2 this error indicator is however an upper bound of the exact solution of (8)–(14) at each step of the discretized NNDD algorithm.

#### 5.3.2 Error Indicator for the NNDD Algorithm

To define a NNDD algorithm error indicator  $\eta^{NN}$ , let us denote by  $(P_h)$  the reference problem defined by finite element discretization of the unilateral contact problem Eqs. (1)–(4) and its solution by  $(\mathbf{d}_h, \mathbf{s}_h)$ . The only approximation introduced between the solution  $(\mathbf{d}_h, \mathbf{s}_h)$  and the finite element solution  $(\mathbf{d}_{p,h}, \mathbf{s}_{p,h})$  is the approximation introduced by the NNDD algorithm. Let  $(\hat{\mathbf{d}}_h, \hat{\mathbf{s}}_h)$  an admissible solution for the problem (35)–(37)

$$\left. \begin{aligned} \hat{\mathbf{u}}_h^\alpha &\in \mathbf{V}_h^\alpha(\mathbf{u}_D^\alpha) \\ \hat{\mathbf{u}}_h^\alpha &= \hat{\mathbf{w}}_h^\alpha, \\ \hat{\mathbf{w}}_h^c &= \hat{\mathbf{w}}_h^1 - \hat{\mathbf{w}}_h^2 \end{aligned} \right\} \text{ on } \Gamma^c. \quad (35)$$

$$\forall \mathbf{v} \in \mathbf{V}_h^\alpha(0), - \int_{\Omega^\alpha} \hat{\boldsymbol{\sigma}}_h^\alpha \boldsymbol{\varepsilon}(\mathbf{v}) dV + \int_{\Gamma_N^\alpha} \mathbf{F}^\alpha \mathbf{v} dS + \int_{\Gamma^c} \hat{\mathbf{t}}_h^\alpha \mathbf{v} dS = 0, \quad (36)$$

$$\int_{\Gamma^c} (\hat{\mathbf{t}}_h^c - \hat{\mathbf{t}}_h^1) \mathbf{v} dS = 0 \quad \text{and} \quad \int_{\Gamma^c} (\hat{\mathbf{t}}_h^c + \hat{\mathbf{t}}_h^2) \mathbf{v} dS = 0 \text{ on } \Gamma^c, \quad (36)$$

$$\hat{\mathbf{q}}_n \leq 0 \text{ and } \mathbf{C} \hat{\Lambda}_n \leq 0 \quad \text{and} \quad \mathbf{C} \hat{\Lambda}_t = 0, \quad (37)$$

where  $\hat{\mathbf{q}}_n$  is the vector of the nodal values of  $\hat{\mathbf{w}}_h^c$ ,  $\hat{\Lambda}_n$  and  $\hat{\Lambda}_t$  are respectively the normal and the tangential components of the nodal values of  $\hat{\mathbf{t}}_h^c$ , and  $\mathbf{C}$  is the contact matrix.

The discretized version  $e_{CRE,h}(\hat{\mathbf{d}}_h, \hat{\mathbf{s}}_h)$  of the error in the constitutive relation defined by Eq. (23) is an error estimator for this reference problem, and is used to define NNDD algorithm error indicator for the unilateral contact problem

$$\eta^{NN} = e_{CRE,h}(\hat{\mathbf{d}}_h, \hat{\mathbf{s}}_h) = \left[ \sum_{\alpha=1}^2 \|\hat{\boldsymbol{\sigma}}_h^\alpha - \mathbf{K}^\alpha \boldsymbol{\varepsilon}(\hat{\mathbf{u}}_h^\alpha)\|_{\boldsymbol{\sigma}, \Omega^\alpha}^2 + 2\hat{\mathbf{q}}_n^T (\mathbf{C} \hat{\Lambda}_n) \right]^{1/2}. \quad (38)$$

## 6 Numerical Results

In this section we give numerical results on two 2D examples. Both examples contain two elastic bodies, one of them clamped along a part of its boundary, whereas the other domain is subject to a non-zero imposed displacement. The results are very similar in the two chosen example, but showing different performances of the NNDD algorithm.

### 6.1 Example 1

The first example is shown on Fig. 2. The lower boundary of structure  $\Omega_1$  is clamped, on structure  $\Omega_2$  the applied force  $F^2$  has a linear distribution ( $F_{max}^2 = 10^7$  Mpa) and the applied displacement is  $u_D^2 = -10^{-4}$  m. The Young's modulus for both structures is  $E = 210$  GPa and the Poisson's ratio is  $\nu = 0.27$ . The coefficient  $\theta$  of the NNDD algorithm is set to 0.25.

To evaluate the computed global estimator, we compute a reference solution denoted by  $\mathbf{u}_{ref}$  and we define the reference error  $e_{ref}$  and the effectivity index  $\gamma$  by

$$e_{ref} = \left[ \sum_{\alpha=1}^2 \|\mathbf{u}_{ref}^\alpha - \mathbf{u}_{h,p}^\alpha\|_{\mathbf{u}, \Omega^\alpha}^2 \right]^{1/2} \quad \text{and} \quad \gamma = \frac{\eta^{glo}}{e_{ref}}. \quad (39)$$

To obtain a reliable reference solution we choose a mesh size  $h_{ref} = 1/8h$  and we set the convergence criteria of the NNDD algorithm to  $\varepsilon_\tau \leq 10^{-8}$ , where we chose to define the precision of the algorithm as

$$\varepsilon_\tau = \frac{2 \max_{\Gamma^c} |\mathbf{t}_p^1 + \mathbf{t}_p^2|}{\max_{\Gamma^c} |\mathbf{t}_p^1| + \max_{\Gamma^c} |\mathbf{t}_p^2|},$$

where  $\mathbf{t}_p^1$  and  $\mathbf{t}_p^2$  are obtained from Step 1 of the NNDD algorithm at iteration  $p$ .

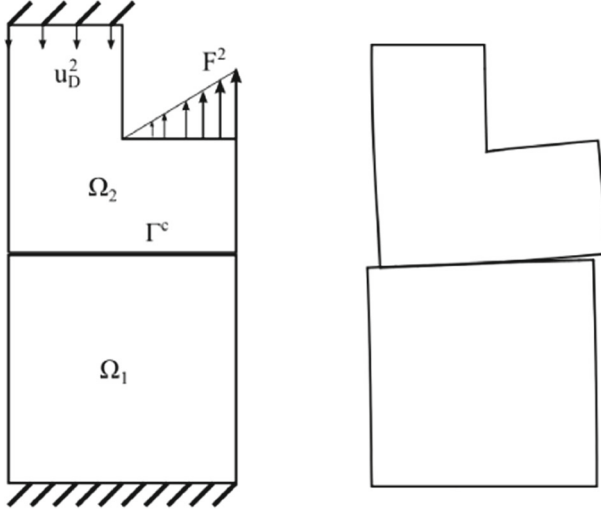


**Fig. 2** Example 1, unilateral contact reference model (*left*)—distorted structures (*right*)

The results are reported in Fig. 3. We have represented the evolution of the effectivity index  $\gamma$  as a function of the number of degrees of freedom ( $n_{DoF}$ ) for a fixed number of iterations of the NNDD algorithm ( $n_{ite} = 3$ ) and its evolution as a function of the number of iterations of the NNDD algorithm for a fixed number of degrees of freedom,  $n_{DoF} = 1,002$ . The results show the upper bound property of the global error estimator. It is worth noticing that the effectivity index seems rather insensitive to the FE discretization as well to the number of iterations.

Figure 4 shows the evolutions of the global error estimator  $\eta^{glo}$ , the FE error indicator  $\eta^{FE}$ , and the NNDD error indicator  $\eta^{NN}$  as functions of the number of iterations of the NNDD algorithm for a fixed number of DoF,  $n_{DoF} = 1,002$ . The global error  $\eta^{glo}$  tends to an horizontal asymptote which is the FE error indicator  $\eta^{FE}$ , whereas the convergence of NNDD error indicator  $\eta^{NN}$  as a function of the number of iterations is shown.

Figure 5 shows the evolution of the global error estimator  $\eta^{glo}$ , of the FE error indicator  $\eta^{FE}$ , and of the NNDD error indicator  $\eta^{NN}$  as a function of the number  $n_{DoF}$  of the degree of freedom (DoF), for a fixed number iterations of the NNDD algorithm  $n_{ite} = 6$  for the example 1. The global error  $\eta^{glo}$  tends to an horizontal asymptote which is the NNDD error indicator  $\eta^{NN}$ , whereas the convergence of FE error indicator  $\eta^{FE}$  as a function of the number of DoF is shown.

The  $\eta^{glo}$  can be numerically related to  $\eta^{NN}$  and  $\eta^{FE}$  by relation (40).

$$\left(\eta^{glo}\right)^2 \approx \left(\eta^{FE}\right)^2 + \left(\eta^{NN}\right)^2. \quad (40)$$

We illustrate the relation (40) in Fig. 6, where are drawn the errors ratio  $r$  as a function of the number of iteration and the number of nodes.

$$r = \frac{\eta^{glo}}{\left[\left(\eta^{FE}\right)^2 + \left(\eta^{NN}\right)^2\right]^{1/2}}.$$

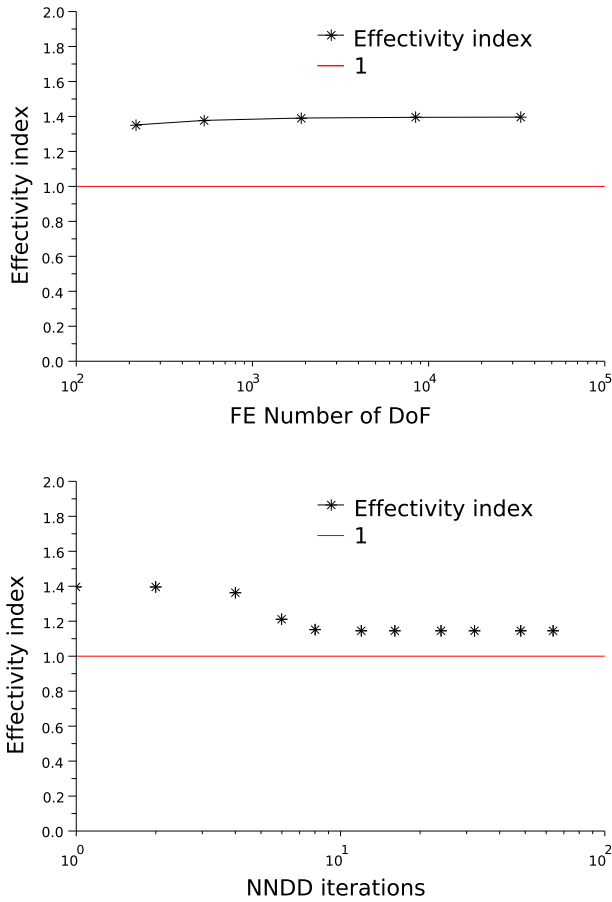


**Fig. 3** Example 1, effectivity index: as a function of the number of DoF (*left*)—as a function of the number of iterations (*right*)

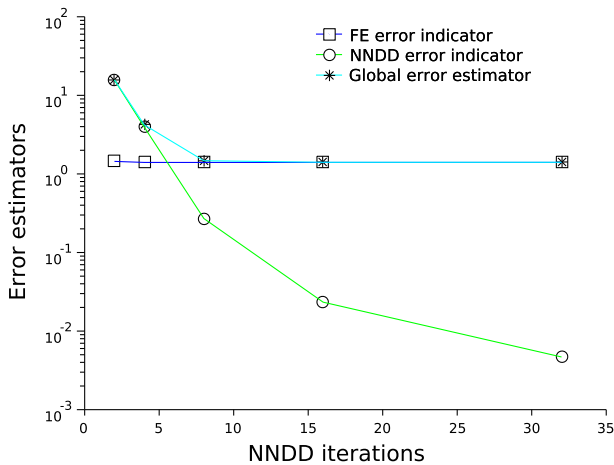


**Fig. 4** Example 1—computed errors as a function of the number iterations of the NNDD algorithm

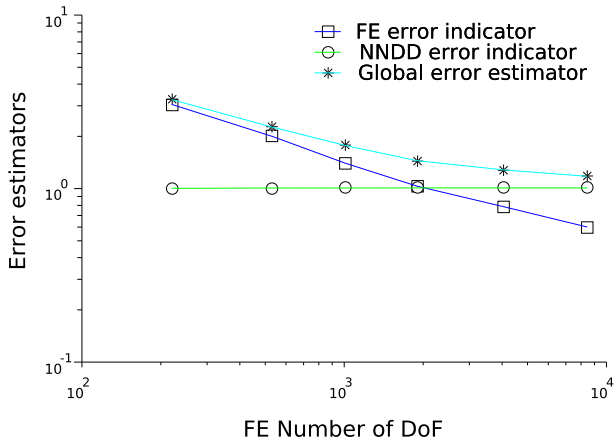


**Fig. 5** Example 1—computed errors as a function of the number of Nodes

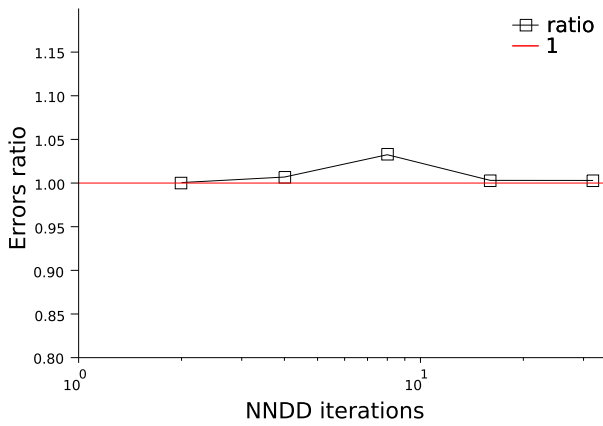
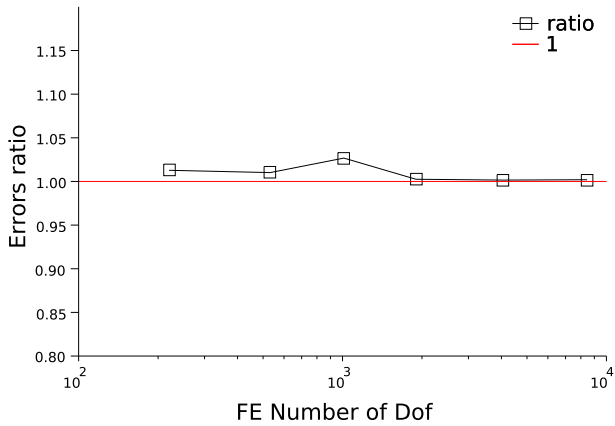


**Fig. 6** Example 1—errors ratio (40)



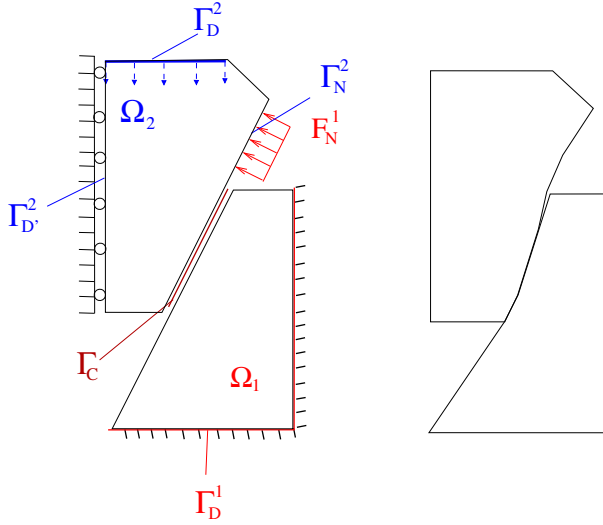


**Fig. 7** Example 2—unilateral contact reference model (*left*)—distorted structures (*right*)

## 6.2 Example 2

The second Example is shown in Fig. 7. The boundary  $\Gamma_D^2$  of domain  $\Omega_2$  is subject to a non-zero imposed displacement whereas the second domain  $\Omega_1$  is clamped along some boundary  $\Gamma_D^1$ . Some superficial forces  $\mathbf{F}_N^1$  are imposed to illustrate loss of contact at the interface. The vertical imposed displacement is set to  $u_D^1 = 10^{-4}$ , the Young's modulus for both structure is set to  $E = 210$  Gpa and the Poisson modula in  $\nu = 0.27$ . The coefficient  $\theta$  of the NNDD algorithm is studied in the range  $[0.2, 0.9]$ .

As for the Example 1, we first study the evolution of the global error estimator  $\eta^{glo}$ , of the FE error indicator  $\eta^{FE}$ , and of the NNDD error indicator  $\eta^{NN}$  as a function of the number  $n_{DoF}$  of the degree of freedom (DoF), for a fixed number iterations of the NNDD algorithm  $n_{ite} = 3$  and a fixed value of the NNDD parameter  $\theta = 0.45$ , which seems “optimal” see Fig. 9. While showing a different performance of the NNDD algorithm for the Example 1, the graphic of Fig. 8 is very similar to Fig. 5. We test the a posteriori error estimates of the NNDD algorithm for different values of  $\theta$ , and two meshes, one coarse mesh with 380 nodes (760 DoF) and one finer mesh with 5,994 nodes (11,992 DoF), for 3 iterations of the algorithm (see Fig. 9). For both meshes, we notice an apparently optimal value near  $0.4 \leq \theta \leq 0.5$ . We also remark that the NNDD algorithm errors are very similar in both fine and coarse meshes. The discretisation errors are naturally greater in the coarse mesh, but it doesn't change much with  $\theta$ .

In Fig. 10 we draw the errors ratio  $r$ , defined in (40), as a function of the parameter  $\theta$  after 3 iterations of the NNDD algorithm on the two different meshes. The figure shows that relation (40) holds for that example.

## 7 Conclusion

A global error estimator has been introduced to verify the finite element approximate solution of an unilateral contact problem computed by a natural Neumann–Neumann domain

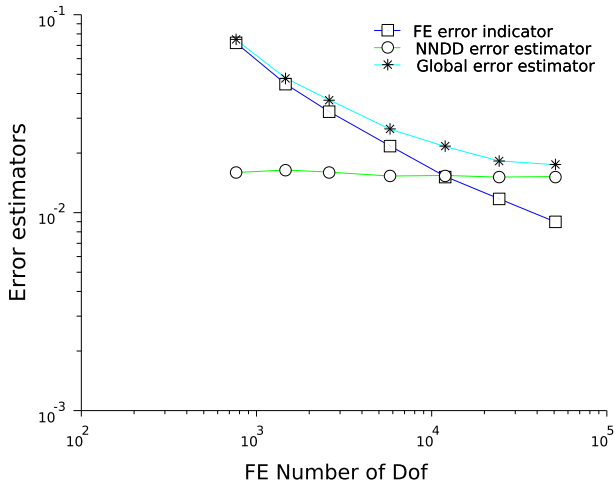


**Fig. 8** Example 2—computed errors as a function of the number of DoF

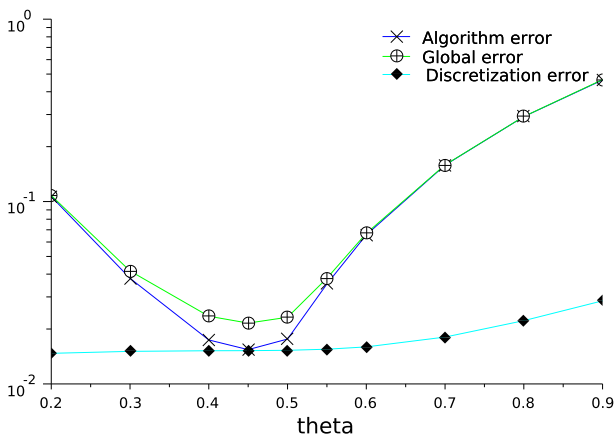
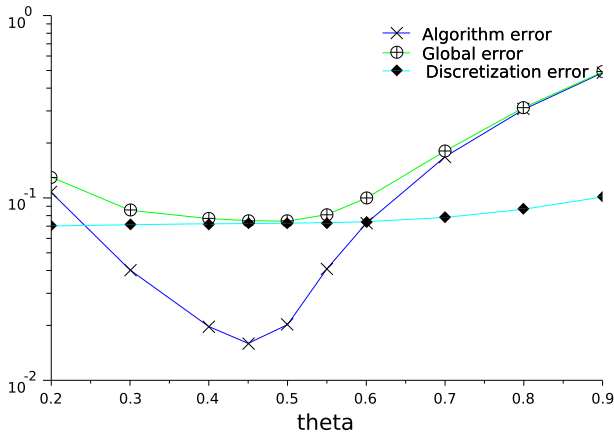


**Fig. 9** Example 2, error indicators for different values of  $\theta$ , coarse 380 nodes mesh (left) and finer 5,994 nodes mesh (right) after 3 iterations

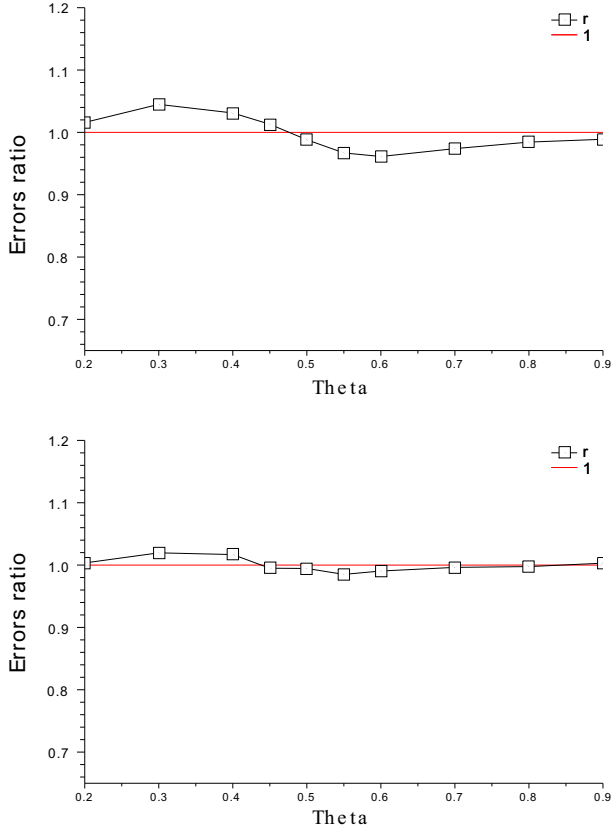


**Fig. 10** Example 2, errors ratio  $r$  as a function of  $\theta$ , coarse mesh (left, 380 nodes) and finer mesh (right, 5,994 nodes) after three iterations of NNDD algorithm

decomposition algorithm. It takes into account all the errors due to discretization, i.e. both the errors due to the space discretization and those due to the domain decomposition algorithm. The proposed error estimator is based on the error in the constitutive relation and on the construction of admissible fields from the finite element solution. The construction of the statically admissible fields is done in three steps: the first step consists in building admissible traction fields on the contact zone, in a second step stress fields that satisfy the FE-equilibrium are recovered, then equilibrated stress fields are computed by a traction free recovery technique. Moreover, two error indicators have been introduced to estimate the error due to either the space discretization or the domain decomposition algorithm solely. The space error indicator is the error in the constitutive relation associated with the reference problem solved at a given iteration of the Neumann–Neumann algorithm. The NNDD algorithm error indicator is the error in the constitutive relation associated with the reference problem solved on a fixed mesh. Satisfactory properties for the indicators have been demonstrated. With these tools, it would be possible to adapt the quality of the mesh during the iterations of the domain decomposition algorithm and to control the final quality of the computation. The extension of these error estimates to other domain decomposition algorithms for unilateral contact problem, such as FETI [26,27] is under consideration.

## References

1. Kikuchi, N., Oden, J.T. (eds.): Contact Problems in Elasticity: A Study of Variational Inequalities and Finite Element Methods. SIAM, Philadelphia (1988)
2. Wriggers, P.: Finite element algorithms for contact problems. *Arch. Comput. Methods Eng.* **2**, 1–49 (1995)
3. Haslinger, J., Hlavacek, I., Necas, J.: Numerical methods for unilateral problems in solid mechanics. In: Ciarlet, P.G., Lions, J.L. (eds.) *Handbook of Numerical Analysis*, vol. IV, part 2. Elsevier, North Holland (1996)
4. Babuška, I., Rheinboldt, W.C.: A posteriori estimates for the finite element method. *Int. J. Numer. Methods Eng.* **12**, 1597–1615 (1978)
5. Ladevèze, P., Leguillon, D.: Error estimate procedure in the finite element method and application. *SIAM J. Numer. Anal.* **20**(3), 485–509 (1983)
6. Zienkiewicz, O.C., Zhu, J.Z.: A simple error estimator and adaptive procedure for practical engineering analysis. *Int. J. Numer. Methods Eng.* **24**, 337–357 (1987)
7. Wriggers, P., Scherf, O.: Different a posteriori error estimators and indicators for contact problems. *Math. Comput. Model.* **28**(4–8), 437–447 (1997)
8. Coorevits, P., Hild, P., Pelle, J.P.: Posteriori error estimation for unilateral contact with matching and non matching meshes. *Comput. Methods Appl. Mech. Eng.* **186**, 65–83 (2000)
9. Rieger, A., Wriggers, P.: Adaptive methods for frictionless contact problems. *Comput. Struct.* **79**, 2197–2208 (2001)
10. Louf, F., Combe, J.P., Pelle, J.P.: Constitutive error estimator for the control of contact problems involving friction. *Comput. Struct.* **81**, 1759–1772 (2003)
11. Louf, F., Gallimard, L., Pelle, J.P.: Un estimateur d'erreur en relation de comportement pour les problèmes d'impact. *Revue Européenne de Mécanique numérique* **15**(6), 699–728 (2006)
12. Bostan, V., Han, W.: A posteriori error analysis for finite element solutions of a frictional contact problem. *Comput. Methods Appl. Mech. Eng.* **195**, 1252–1274 (2006)
13. Wohlmuth, B.I.: An a posteriori error estimator for two-body contact problems on non-matching meshes. *J. Sci. Comput.* **33**(1), 25–45 (2007)
14. Gallimard, L., Sassi, T.: A posteriori error analysis of a domain decomposition algorithm for unilateral contact problem. *Comput. Struct.* **88**, 879–888 (2010)
15. Farhat, C., Lesoinne, M., LeTallec, P., Pierson, K., Rixen, D.: FETI-DP : a dual-primal unified FETI method. I. A faster alternative to the two-level FETI method. *Int. J. Numer. Methods Eng.* **50**(7), 1523–1544 (2001)
16. Mandel, J.: Balancing domain decomposition. *Commun. Appl. Numer. Methods Eng.* **9**, 233–241 (1993)
17. Parret-Fraud, A., Rey, C., Gosselet, P., Feyel, F.: Fast estimation of discretization error for FE problems solved by domain decomposition. *Comput. Methods Appl. Mech. Eng.* **199**(49–52), 3315–3323 (2010)
18. Bayada, G., Sabil, J., Sassi, T.: A Neumann–Neumann Domain Decomposition algorithm for the Signorini problem. *Appl. Math. Lett.* **17**, 1153–1159 (2004)
19. Haslinger, J., Kucera, R., Sassi, T.: A domain decomposition algorithm for contact problems: analysis and implementation. *Math. Model. Nat. Phenom.* **4**(1), 123–146 (2009)
20. De Saxcé, G.: A generalisation of Fenchel's inequality and its applications to the constitutive laws. *C.R. Acad. Sci. Paris Série II* **314**, 125–129 (1992)
21. Prager, W., Synge, J.L.: Approximation in elasticity based on the concept of functions space. *Q. Appl. Math.* **5**, 261–269 (1947)
22. Gallimard, L.: A constitutive relation error estimator based on traction-free recovery of the equilibrated stress. *Int. J. Numer. Methods Eng.* **78**, 460–482 (2009)
23. Gallimard, L., Ladevèze, P., Pelle, J.P.: Error estimation and time–space parameters optimization for FEM non linear computation. *Comput. Struct.* **64**(1–4), 145–156 (1997)
24. Ladevèze, P., Moes, N.: Adaptive control for finite element analysis in plasticity. *Comput. Struct.* **73**, 45–60 (1999)
25. Pelle, J.P., Ryckelynck, D.: An efficient adaptive strategy to master the global quality of viscoplastic analysis. *Comput. Struct.* **78**(1–3), 169–183 (2000)
26. Dureisseix, D., Farhat, C.: A numerically scalable domain decomposition method for the solution of frictionless contact problems. *Int. J. Numer. Methods Eng.* **50**(12), 2643–2666 (2001)
27. Dureisseix, D., Farhat, C.: A FETI-based algorithm for the iterative solution of unilateral contact problems. In: 4th Euromech Solids Mechanics Conference—Metz (2000)